Journal of Radiation Research, Vol. 57, No. 2, 2016, pp. 133–141
doi: 10.1093/jrr/rrv077
Advance Access Publication: 24 December 2015

Radiation-induced lung fibrosis in a tumor-bearing mouse model is associated with enhanced Type-2 immunity

Jing Chen[1,2], Yacheng Wang[1,2], Zijie Mei[1,2], Shimin Zhang[1,2], Jie Yang[1,2], Xin Li[1,2], Ye Yao[1,2] and Conghua Xie[1,2*]

[1]Department of Radiation and Medical Oncology, Zhongnan Hospital, Wuhan University, 169 Dong Hu Road, Wuhan, Hubei 430071, P.R. China
[2]Hubei Key Laboratory of Tumor Biological Behaviors, Zhongnan Hospital, Wuhan University, 169 Dong Hu Road, Wuhan, Hubei 430071, P.R. China
*Corresponding author. Department of Radiation and Medical Oncology and Hubei Key Laboratory of Tumor Biological Behaviors, Zhongnan Hospital, Wuhan University, 169 Dong Hu Road, Wuhan, Hubei 430071, P.R. China. Tel: +86-27-67812607; Fax: +86-27-67812684; Email: chxie_65@hotmail.com
Received March 14, 2015; Revised September 16, 2015; Accepted October 9, 2015

ABSTRACT

Lung fibrosis may be associated with Type-2 polarized inflammation. Herein, we aim to investigate whether radiation can initiate a Type-2 immune response and contribute to the progression of pulmonary fibrosis in tumor-bearing animals. We developed a tumor-bearing mouse model with Lewis lung cancer to receive either radiation therapy alone or radiation combined with Th1 immunomodulator unmethylated cytosine-phosphorothioate-guanine containing oligodeoxynucleotide (CpG-ODN). The Type-2 immune phenotype in tumors and the histological grade of lung fibrosis were evaluated in mice sacrificed three weeks after irradiation. Mouse lung tissues were analyzed for hydroxyproline and the expression of Type-1/Type-2 key transcription factors (T-bet/GATA-3). The concentration of Type-1/Type-2 cytokines in serum was measured by cytometric bead array. Lung fibrosis was observed to be more serious in tumor-bearing mice than in normal mice post-irradiation. The fibrosis score in irradiated tumor-bearing mice on Day 21 was 4.33 ± 0.82, which was higher than that of normal mice (2.00 ± 0.63; $P < 0.05$). Hydroxyproline and GATA-3 expression were increased in the lung tissues of tumor-bearing mice following irradiation. CpG-ODN attenuated fibrosis by markedly decreasing GATA-3 expression. Serum IL-13 and IL-5 were elevated, whereas INF-γ and IL-12 expression were decreased in irradiated tumor-bearing mice. These changes were reversed after CpG-ODN treatment. Thus, Type-2 immunity in tumors appeared to affect the outcome of radiation damage and might be of interest for future studies on developing approaches in which Type-1–related immunotherapy and radiotherapy are used in combination.

KEYWORDS: tumor-bearing, Type-1/Type-2, immune imbalance, radiation-induced lung injury, fibrosis

INTRODUCTION

Radiation-induced lung injury (RILI) is one of the most common and dose-limiting side-effects of thoracic radiotherapy, which compromises the success of lung cancer treatments [1]. Approximately 10% to 20% of patients with non–small cell lung cancer (NSCLC) who receive definitive radiation therapy experience clinically severe RILI (Grade ≥3) [2–4]. In most cases, pathological changes resulting from RILI eventually lead to lung fibrosis [5, 6]. Although the mechanism(s) underlying the pathogenesis of radiation-induced lung fibrosis (RILF) at the molecular and cellular levels is not yet fully understood, initial immune and inflammatory responses to repeated stimuli lead to tissue injury and progressive fibrosis [7].

Radiation therapy can stimulate immunological activity in both tumor and non-tumor microenvironments. Radiation activates inflammation and immunity through initiation of lymphocyte infiltration, in particular the recruitment of T cells [7–10]. T-helper Type 1 (Th1) and 2 cells (Th2), are differentiated from naive CD4+ T (Th0) cells. The differentiation of Th0 cells into Th1 or Th2 cells is regulated by the transcription factors (i) T-box expressed in T-cells (T-bet) and (ii) GATA-binding protein-3 (GATA-3). Th1 cells predominantly

produce cytokines such as interleukin (IL)-2 and interferon-gamma (IFN-γ), and Th2 cells produce IL-4, IL-5 and IL-13 [11, 12]. Studies have shown, in a range of fibrosis disease models, that Type-2 cytokines such as IL-4 and IL-13 enhance fibrotic processes by activating fibroblast proliferation and collagen production, whereas Type-1 cytokines inhibit these processes [13–15]. In our previous study, we also observed high levels of Type-2 cytokines in healthy mice with RILF [14]. GATA-3 expression in irradiated lung tissues upregulated alternatively activated macrophages (M2 macrophages) which express high levels of arginase-1 as a result of lung fibrosis [14]. Thus, different Type-1/Type-2 immune system function could be related to more progressive fibrosis.

Tumor cells produce immunosuppressive cytokines that impair anti-tumor immune responses [16, 17]. Recent reports have shown that some Type-2 cytokines such as IL-4, IL-5, IL-10 and IL-13 are expressed in lung cancer cell lines, whereas there is little expression of Type-1 cytokines [18, 19]. Similarly, peripheral blood lymphocytes isolated from patients with NSCLC produce high levels of IL-10 but low levels of IFN-γ [20]. Both lung tissue and peripheral blood T cells isolated from NSCLC patients have low levels of T-bet expression [21, 22]. Furthermore, even in the absence of clinical or radiographic findings, the lung parenchyma contralateral to the tumor suffers an early and significant increase in interstitial fibrosis (thickness) and congestion after radiation therapy, as monitored by serial transbronchial biopsy [23]. These observations suggest that NSCLC may be characterized by a Type-2–biased immune phenotype and likely promotes the formation of fibrotic tissue. However, current knowledge of RILF biology is mainly limited to patients with a normal status, and further *in vivo* investigations using tumor models are required.

In order to determine whether irradiated lung tissue aggravates lung fibrosis in a tumor model, we subjected mice with lung cancer to X-ray irradiation and assessed Type-2 immunity and the degree of lung fibrosis. In addition, we examined whether suppressing Type-2 immunity could delay RILF by using a Type-1 immunologic adjuvant, CpG-ODN. These data might provide a better understanding of the role of constitutive host immunity on radiation-induced tissue damage.

MATERIALS AND METHODS

Mice

Female C57BL/6 mice (6–8 weeks old; weight, 18–22 g) were purchased from the Animal Center of Wuhan University. Animals were maintained in an environment with 60 ± 5% humidity and 25 ± 1°C under a 12 h light–dark cycle. All experimental animals were housed under specific pathogen-free conditions for 1 week prior to the initiation of the experiments. The experimental protocols were approved by the Medical Sciences Animal Care Committee of Hubei Province, China.

The mice ($n = 6$ for each time-point per group) were divided into six experimental groups as follows: (i) CTL group: healthy mice without any treatment; (ii) LW group: tumor-bearing mice without any treatment; (iii) radiotherapy (RT) group: healthy mice that received radiation; (iv) LRT group: tumor-bearing mice that received radiation. (v) C group: tumor-bearing mice that received only Th1 immunomodulation; (vi) CRT group: tumor-bearing mice that received both radiation and Th1 immunomodulation.

Mouse tumor model

3LL tumor cells (LLC cells) were used for development of the mouse tumor model and subsequent *in vivo* evaluation of the Type-1/Type-2 cytokine profile. Tumor cells were cultured and inoculated subcutaneously into the right armpit of each C57BL/6 mouse at a concentration of 5×10^3 cells. The growth rate of the tumor and the tumor size were measured every 2 days by measuring the length of two perpendicular dimensions. The volume of each tumor was calculated using the following formula: volume = $0.5 \times \text{length} \times \text{width}^2$. When the tumors reached a size of 100 mm^3, the animals were randomly assigned to the LW, LRT, C or CRT group. Blood samples were collected before treatment and at 0, 1, 3, 7, 14 or 21 days post-irradiation, and serum was separated by centrifugation. Mice were sacrificed by cervical dislocation. Sera were stored at –70°C and other specimens were stored in liquid nitrogen until further analysis.

Radiation treatment regimen

A plastic jig was used to restrain the mice without anesthesia, and lead blocks were placed to shield the head and abdomen. A total of 12 Gy was administered to the mid-plane of the lungs in a single dose via a posterior field using a linear accelerator (Siemens Primus-Hi). The beam was of 6-MV photons at a dose rate of 1.886 Gy/min, the source–surface distance (SSD) was 1 m, and the size of the radiation field was 2.5 × 15 cm. The RT field involved both the armpit and the whole lung. The depth of the maximum dose of the radiation was significantly reduced by the tissue-equivalent plastic material (10-mm thickness) of the restraining jig. Film dosimetry was used to determine the relative dose distribution and dosimetry was performed using a cylindrical ionization chamber. Following irradiation, the mice were maintained in a specific pathogen-free environment and provided with a standard diet and water.

Treatment of mice with Type-1 immunomodulator CpG-ODN

CpG-ODN can selectively activate Type-1 immunity. CpG-ODN was synthesized by Beijing Tianyi Huiyuan Bioscience and Technology Inc. (Beijing, China). The CpG-ODN sequence used in this study was 5′-TCCATGACGTTCCTGACGTT-3′. The ODN was diluted with phosphate-buffered saline (PBS) to a final concentration of 250 mg/ml and stored at 4°C. Mice were treated with either 0.2 ml CpG-ODN (250 μg/ml) or 0.2 ml PBS via intraperitoneal injection, and treatments were administered 30 min, 24 h and 48 h after irradiation. The irradiated tumor-bearing mice treated with CpG-ODN were assigned to the CRT group.

Tissue isolation

Mice were sacrificed by cervical dislocation before irradiation (Day 0) and 1, 3, 7, 14 or 21 days post-irradiation. The left lung lobes were excised for histological examination and were also used to measure the hydroxyproline content (see below). The right lung lobes were snap-frozen in liquid nitrogen and later used for RNA and protein isolation. Sera samples were analyzed by Cytometric Bead Array.

Lung and tumor tissue histopathology

Paraffin-embedded tissues were sectioned to an average thickness of 4 μm. Lung tissues were stained with hematoxylin and eosin (H&E)

to determine histological changes, and Masson's stain was used to detect collagen. Tumor tissues were stained for immunohistochemical analysis of T-bet and GATA-3. The fibrosis score was evaluated by two independent investigators, in a blinded manner, according to the criteria of Hübner *et al.* [24]. The fibrosis score was obtained from partial left lung lobes. Collagen content was determined indirectly by assessing hydroxyproline levels in the remaining portion of the left lung. An alkaline hydrolysis assay kit (Jiancheng Biological Institution, Nanjing, China) was used to measure hydroxyproline content, according to the manufacturer's instructions. The quantity of hydroxyproline was determined based on the following formula: content of hydroxyproline (μg/mg, wet weight) = [absorbance (sample) – absorbance (blank)]/[absorbance (standard) – absorbance (blank)] × 5 μg/ml × 10 ml/wet weight (tissue).

RT-PCR analysis

Total RNA was extracted using TRIzol reagent (Invitrogen, Carlsbad, CA, USA) according to the manufacturer's protocol. Polymerase chain reaction (PCR) primers for murine *GATA-3*, *T-bet* and the housekeeping gene *β-actin* were designed by ShineGene Co. Ltd, based on cDNA sequences obtained from the GenBank database. Briefly, cDNA was synthesized from 2 μg of total RNA using the Revert Aid^{TM} fist strand cDNA Synthesis Kit (Fermentas, Hanover, MD, USA). DNA primer sequences were as follows: *β-actin*: 5′-TGGAAGGACTCATGACCACA-3′ (forward) and 5′- CCTGCTTC ACCACCTTCTTGA-3′ (reverse); *T-bet*: 5′-CCCAGCCGTTTC TACCCC-3′ (forward) and 5′-TCGGAACTCCGCTTCATAACT-3′ (reverse); *GATA-3*: 5′-ACTGCGGGGCAACCTCTA-3′ (forward) and 5′-CGGTTCTGCCCATTCATTTT-3′ (reverse). The amplification conditions were 94°C for 5 min followed by 35 cycles of 94°C for 30 s, 60°C for 30 s and 72°C for 30 s, with an additional extensions step for 7 min at 72°C. *T-bet* and *GATA-3* mRNA expression was normalized to *β-actin*. For example, relevant mRNA expression (e) = 2 – (C_t of test – C_t of *β-actin*), where C_t represents the cycle threshold for amplification. All experiments were repeated at least three times.

Western blot analysis

Lung tissue samples were homogenized in cold cell lysate radioimmunoprecipitation assay buffer (RIPA, Sigma–Aldrich, Shanghai, China), and the protein concentration was determined using the micro-BCA kit (Applygen Technologies Inc., Beijing, China). Equal amounts of protein (50 μg/condition) from individual mice in each group were separated by electrophoresis on an 8–10% SDS-PAGE gel, and then electrotransfered to polyvinylidene fluoride (PVDF, Millipore) membranes. The membranes were blocked with blocking buffer (BSA, pH7.5) for 1 h at room temperature. The blots were then incubated overnight at 4°C with GATA-3 (200 μg/ml) or T-bet (200 μg/ml) specific primary antibodies, with β-actin (100 μg/ml) used as an internal control. All primary antibodies were purchased from Santa Cruz Biotechnology. After washing with TBS-T buffer, the blots were incubated with horseradish peroxidase–conjugated anti-rabbit IgG antibodies (1 : 3000 dilution in TBS-T) at room temperature for 1 h and washed with TBS-T buffer for 30 min. Finally, the reaction was visualized using a chemiluminescence reagent kit (BioTime, Beijing, China) and exposed to X-ray film (Kodak Scientific Imaging Systems).

Enzyme-linked immunosorbent assay (ELISA)

The concentrations of STAT1, STAT4 and STAT6 in murine lung tissues from the LRT group and the CRT group were measured using a commercial quantitative sandwich ELISA kit (Elabscience Biotechnology Co., China) according to the manufacturer's instructions. Concentrations were estimated from a standard curve and expressed as ng/ml. The ELISA kit was able to detect a minimum of 0.1 ng/ml of protein.

Measurement of serum cytokines

Murine serum was collected from euthanized mice at various timepoints post irradiation. A Cytometric Bead Array (CBA) specific for mouse Type-1/Type-2 cytokines (BD Biosciences, San Diego, CA) was used to measure the amount of IFN-γ, IL-12, IL-5 and IL-13 production, according to the manufacturer's instructions. Briefly, microbead populations with distinct fluorescence signals were coated with capture antibodies specific for each cytokine. The capture beads, phycoerythrin-conjugated detection antibodies, and test samples (recombinant standards used to generate a standard curve) were incubated at room temperature, and the samples were subsequently washed with 1 ml of wash buffer and pelleted by centrifugation (200 *g* for 5 min). After careful aspiration of the supernatant, the beads were resuspended in 300 μl wash buffer, vortexed briefly, and analyzed on a BD FACScan using BD CBA analysis software. Each assay had a sensitivity range of 20 to 5000 pg/ml.

Statistical analysis

Statistical analysis was performed using GraphPad InStat 3.06 (GraphPad Software, San Diego, CA, USA). All data were expressed as the mean ± SD. Intergroup comparisons were performed using one-way ANOVA, and *P* values less than 0.05 were considered statistically significant.

RESULTS

Characterization of Type-2 immune phenotype in the tumor-bearing mouse model

Lewis lung carcinoma cells were successfully implanted ∼1 week after inoculation. The tumor-bearing mice were randomly assigned to the LW, LRT, C or CRT groups, while healthy mice were assigned to the CTL or RT groups (see Materials and Methods for a definition of each group.).

Prior to treatment, Type-1/Type-2 cytokine plasma levels were found to differ between healthy mice and tumor-bearing mice. As shown in Fig. 1A, serum IL-13 production in tumor-bearing mice from the LW group was much higher than that in the CTL mice (8.31 ± 1.11 pg/ml and 2.25 ± 1.16 pg/ml, respectively), whereas the levels of IFN-γ and IL-12 were significantly decreased ($P < 0.05$) when compared with mice in the CTL group. To evaluate whether the Type-2 immune phenotype was altered in tumor-bearing mice after irradiation, we performed western blot and immunohistochemical analysis using anti-GATA-3 and anti-T-bet antibodies. We found high levels of GATA-3 expression and relatively low levels of T-bet expression in the tumor masses from mice in the LRT group (Fig. 1B). Gray scanning analysis showed that GATA-3 expression was not significantly altered after irradiation. Histological analysis demonstrated that the percentage of the mean intensity of GATA-3 and T-bet in tumors from LW mice before irradiation was

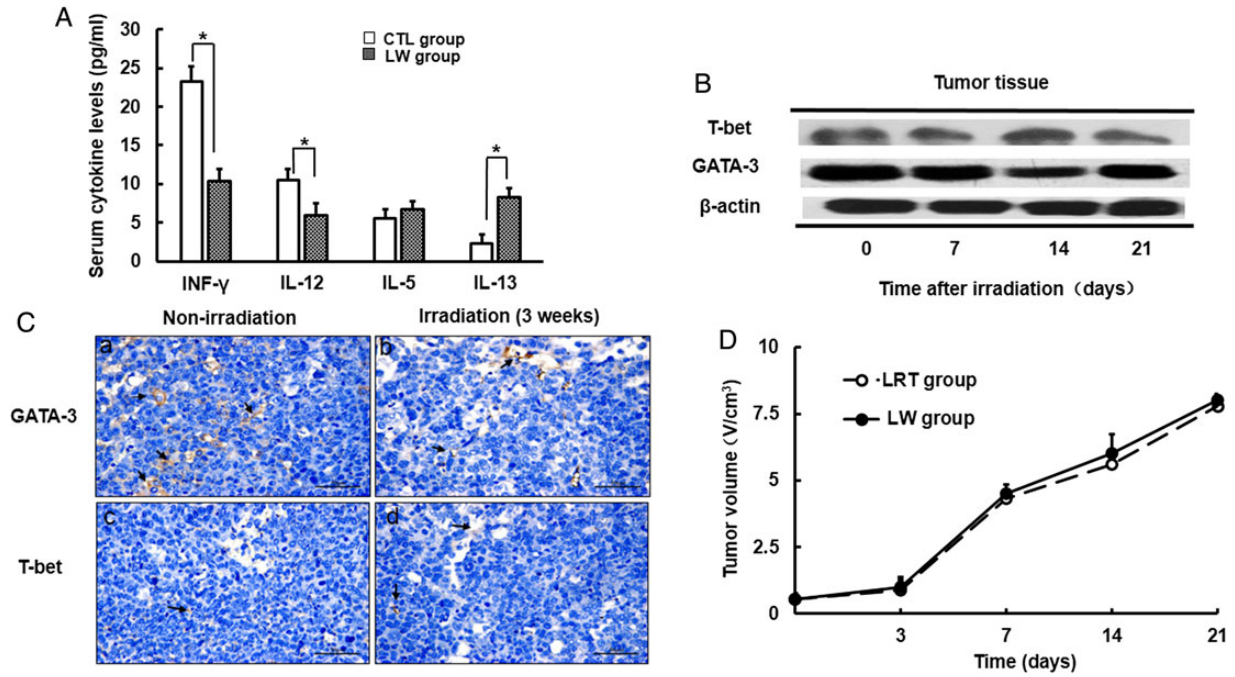

Fig. 1. Characterization of Type-2 immune response in the tumor-bearing mouse model. (A) Differences in serum Type-1/2 cytokine levels between CTL group and LW group mice. (B) The expression of T-bet/GATA-3 in tumors before and after irradiation was measured by western blot. (C) T-bet and GATA-3 expression in tumors was detected by immunohistochemistry (magnification × 400). A representative picture is shown here. Arrows indicate positive expression. (D) Differences in tumor growth curves between LW group and LRT group mice. Data are shown as the mean ± SD. *$P < 0.05$. CTL group: healthy mice without any treatment; LW group: tumor-bearing mice without any treatment.

342.61 ± 21.31 and 27.34 ± 11.31, respectively (Fig. 1C). The percentage was not significantly changed after irradiation (328.31 ± 41.54 and 32.25 ± 17.16, respectively; $P > 0.05$). Tumor shrinkage was not observed when comparing non-irradiated with irradiated tumor-bearing mice (Fig. 1B and D).

CpG-ODN treatment enhanced Type-1 immune response and caused tumor regression in the tumor-bearing mouse model

Tumor-bearing mice that had been treated with CpG-ODN for 3 weeks had significantly increased serum levels of IFN-γ and IL-12 and reduced serum levels of IL-5 and IL-13 (Fig. 2A). In Fig. 2B, at Day 14 after irradiation, the volumes of tumor masses were much smaller in the CRT group mice ($t = 6.29$, $P < 0.05$) compared with in mice from the LRT group. Increased tumor regression was observed in mice treated with a combination of irradiation and CpG-ODN compared with those treated with CpG-ODN administration alone ($t = 6.33$, $P < 0.05$). This phenomenon of tumor regression was gradually enhanced over time.

Increasing lung fibrosis in tumor-bearing mice after irradiation

An increase in interstitial lung fibrosis was observed 3 weeks after exposure to 12 Gy of X-rays (Fig. 3A). Large collagen deposits were also observed in the alveolar septa and bronchiolar area, with obliteration of the alveoli (Fig. 3A). At each time-point, the mean fibrosis score in the LRT group was higher than in the other two groups of irradiated mice (Table 1). A significant difference between the groups was found in terms of the fibrosis score at 3 weeks after irradiation ($P < 0.05$).

As an indicator of the severity of pulmonary fibrosis, the hydroxyproline content in the lungs was analyzed. The hydroxyproline content in the lungs of the LRT group mice was higher than in mice from the RT group ($P < 0.05$). Compared with the RT group, the tumor-bearing mice in the LRT group had significantly increased hydroxyproline levels 3 weeks post irradiation (0.312 ± 0.02 and 0.434 ± 0.04 μg/mg; $P < 0.01$; Fig. 3B).

T-bet and *GATA-3* mRNA and protein expressions in mouse lungs

To explore the role of Type-1/Type-2 immune status in RILF, the remaining lung sections were collected for Real time (RT) - PCR (RT-PCR) and western blot analysis. Relative *T-bet* and *GATA-3* mRNA expression are shown in Fig. 4A and B, respectively. Overall, the level of *T-bet* in the RT group was higher over the 3-week experimental period compared with in the LRT group, and reached a maximum at 2 weeks post irradiation (1.71 ± 0.28, and 0.31 ± 0.10; $P < 0.05$; Fig. 4A). In contrast, tumor-bearing mice from the LRT group typically had higher levels of *GATA-3*, particularly 1 week post irradiation, when compared with mice in the RT group ($P < 0.05$; Fig. 4B).

In accordance with the results obtained from the RT-PCR analysis, GATA-3 protein levels also showed a time-dependent increase in both the LRT and RT groups. Higher levels of GATA-3 were

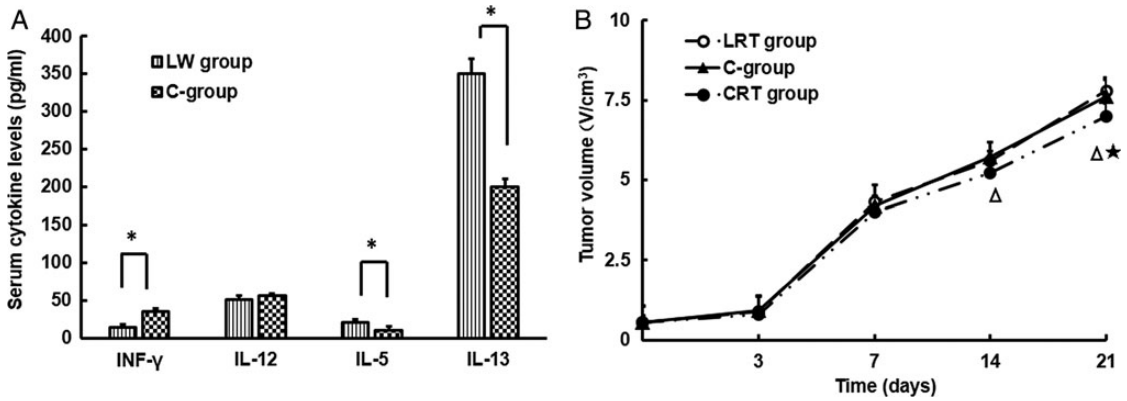

Fig. 2. Anti-tumor response of CpG-ODN treatment. (A) Differences in serum Type-1/2 cytokine levels between LW group and C-group mice. Data are shown as the mean ± SD. *$P < 0.05$. (B) Tumor growth curves for LRT group, C-group and CRT group mice. Data are shown as the mean ± SD. CRT group vs LRT group, $P < 0.05$; CRT group vs C-group, $P < 0.05$; LRT group: tumor-bearing mice that received radiation (open circles); C-group: tumor-bearing mice that only received Th1 immunomodulation (filled triangles); CRT group: tumor-bearing mice that received both radiation and Th1 immunomodulation (closed circles).

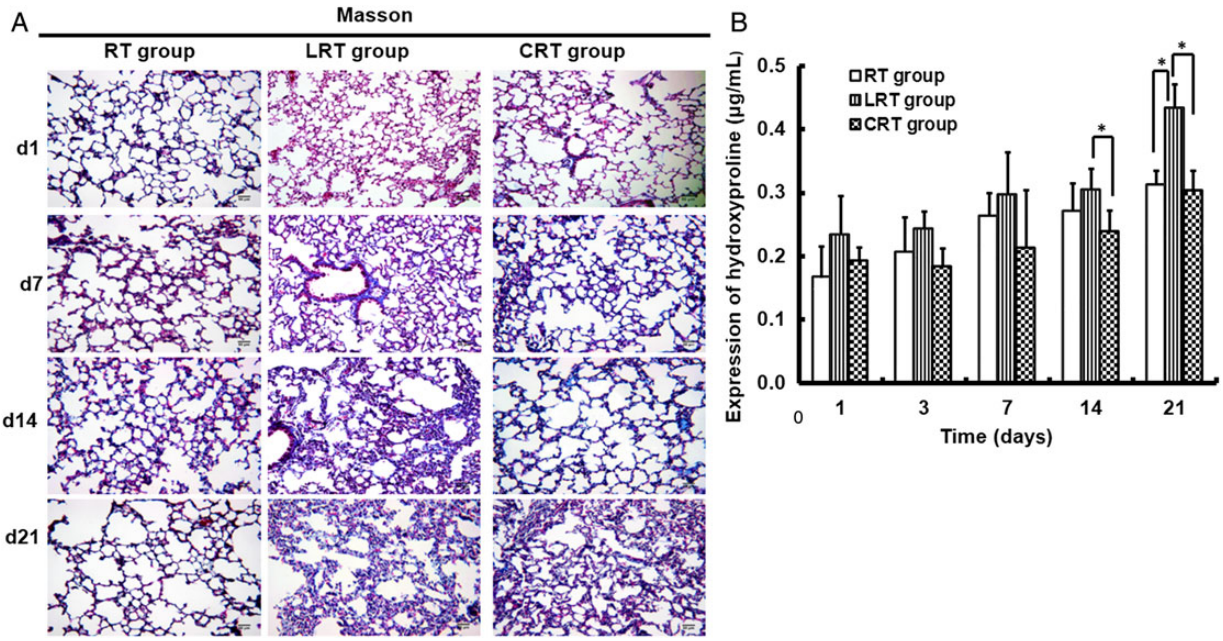

Fig. 3. Pathological features of radiation-induced lung fibrosis in mouse lung tissues. Representative slides indicate lungs from LRT, RT and CRT group mice. Lung tissue sections obtained on Days 1, 7, 14 and 21 after irradiation. (A) Masson's staining for collagen in mouse lung tissues (magnification × 20). Collagen fibers were stained blue. (B) Comparison of hydroxyproline expression in mouse lung tissues after irradiation. Data are shown as mean ± SD. *$P < 0.05$.

observed in the LRT group compared with in the RT group. The expression of T-bet in the LRT group gradually decreased to the lowest level 3 weeks after irradiation (Fig. 4C).

CpG-ODN significantly delayed the development of lung fibrosis after irradiation

To examine changes in lung tissue after thoracic irradiation combined with CpG-ODN treatment, the extent of fibrosis in individual mouse lungs was assessed histologically 3 weeks after radiation. Histological assessment revealed a decrease in the alveolar septum thickness in mice from the CRT group (Fig. 3A). The fibrosis score significantly decreased after CpG-ODN treatment, both at 14 and 21 days post-irradiation (Table 1). Meanwhile, the amounts of hydroxyproline at each time-point after irradiation were lower than in mice in the LRT group ($P < 0.05$; Fig. 3B).

Table 1. Fibrosis score according to groups

Groups	Fibrosis score									
	d1		d3		d7		d14		d21	
	Mean ± SD	Range	Mean ± SD	Range	Mean ± SD	Range	Mean ± SD	Range	Mean ± SD	Range
RT group	1.33 ± 0.52	1–2	1.50 ± 0.54	1–2	1.83 ± 0.41	1–2	2.00 ± 0.89	1–3	2.00 ± 0.63	1–3
LRT group	1.67 ± 0.52	1–2	1.83 ± 0.41	1–2	2.33 ± 1.03	1–4	3.33 ± 1.21	2–5	4.33 ± 0.82	3–5
CRT group	1.50 ± 0.55	1–2	1.67 ± 0.52	1–2	2.00 ± 0.89	1–3	2.17 ± 0.98	1–4	3.00 ± 0.89	2–4

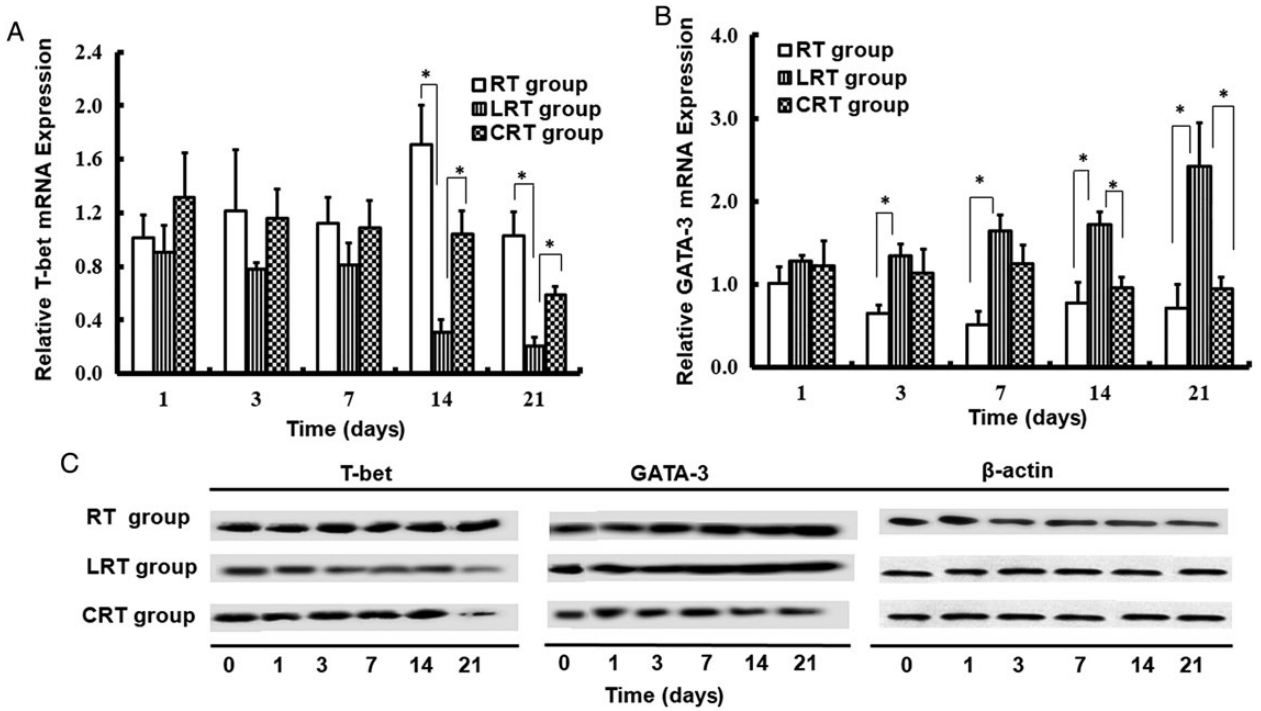

Fig. 4. Expression of transcription factors for Type-1/Type-2 immune response up to 21 days. *T-bet* (A) and *GATA-3* (B) mRNA expression in RT group, LRT group and CRT group mice was measured by RT-PCR. (C) The difference between T-bet and GATA-3 protein expression was measured by western blot. Data are shown as mean ± SD. *$P < 0.05$.

Activation of STAT-1 and STAT-4 expression, but inhibition of STAT-6 may be the underlying mechanism in lung fibrosis mitigation as a result of CpG-ODN administration

STAT-1, STAT-4 and STAT-6 are the main upstream factors of T-bet and GATA-3 that play pivotal roles in activating the Type-1 and Type-2 cytokine pathways. Therefore, using an ELISA, we examined whether the expression of STAT-1, STAT-4 and STAT-6 protein in lungs could be regulated by CpG-ODN. Decreased GATA-3 expression and increased T-bet levels were noted after administration of CpG-ODN to tumor-bearing mice after irradiation (Fig. 4). ELISA tests further revealed that STAT1 expression in irradiation lung tissue from CRT group mice increased quickly after one week of CpG-ODN treatment ($P < 0.05$; Fig. 5A). Then, After 3 weeks CpG-ODN administration, the levels of STAT1 and STAT4 in lung tissue from CRT group mice were both significantly increased compared with in lung tissue from LRT group mice ($P < 0.05$; Fig. 5A and B). Contrarily, the STAT6 expression was sharply decreased ($P < 0.05$; Fig. 5C).

Changes in Type-1/Type-2 cytokine plasma levels after irradiation

High levels of Type-1 cytokines (IFN-γ and IL-12) were observed in mice from the RT group, especially at Day 14 (IFN-γ, 298 ± 2.52 pg/ml; IL-12, 600 ± 0.30 pg/ml) (Fig. 6A and B). The expression of these cytokines was lower in the LRT group than in the RT group. Serum IFN-γ and IL-12 levels in the LRT group decreased rapidly to a minimum and were much lower compared with those of the RT group (P <0.05; Fig. 6A and B). In contrast, high levels of Type-2 cytokines (IL-5 and IL-13) were present in mice from the LRT group (Fig. 6C and D). The highest level of IL-13 and IL-5 expression was 350 ± 0.43 pg/ml and 20.5 ± 0.39 pg/ml, respectively, at 3 weeks post irradiation ($P < 0.05$; Fig. 6C and D). When the mice were treated

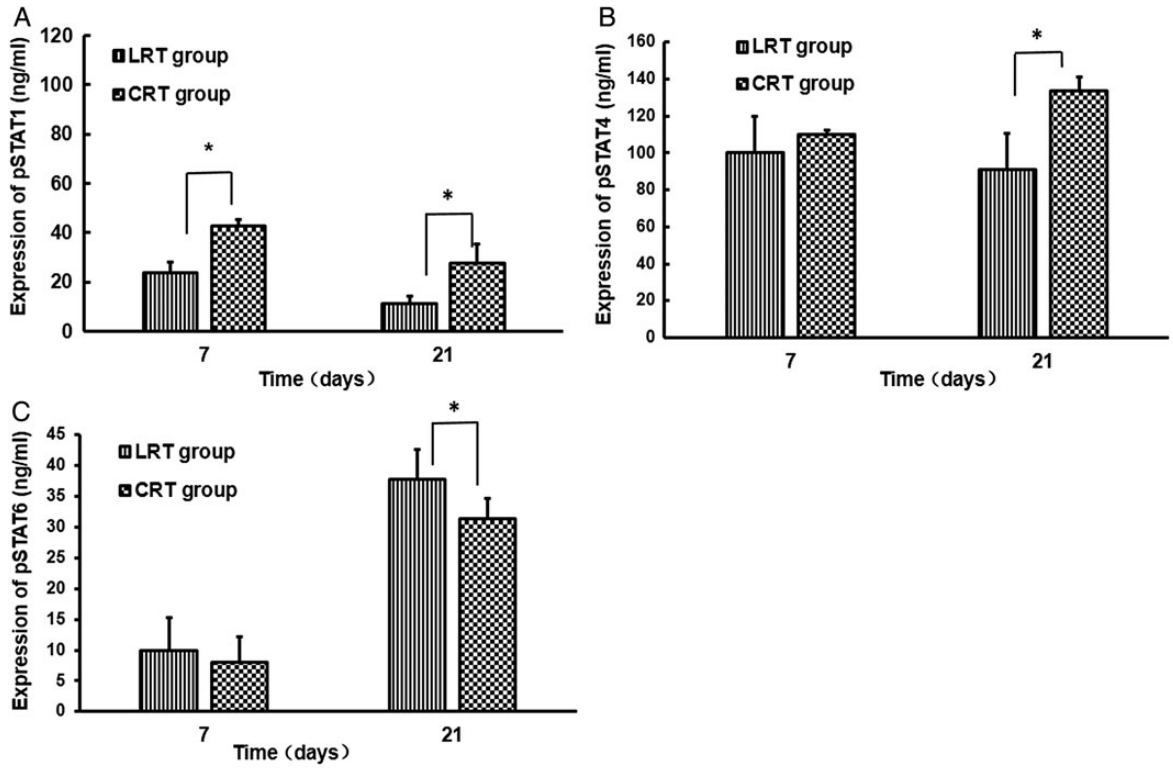

Fig. 5. Effects of CpG-ODN on the expression of phosphorylated (p) -STAT1, pSTAT4 and pSTAT6 proteins in lung tissues after irradiation. STAT1, STAT4 and STAT6 are signal transduction molecules associated with IFN-γ, IL-12 and IL-4/IL-13 receptors, respectively. Data are shown as mean ± SD. Compared with LRT group: *$P < 0.05$.

with CpG-ODN, serum IL-12 and INF-γ levels increased in the CRT group at Day 7 and 14 compared with in the LRT group, whereas IL-5 and IL-13 levels decreased sharply ($P < 0.01$; Fig. 6).

DISCUSSION

We previously reported that radiation-induced lung fibrosis, a common and late complication of thoracic radiotherapy, was related to a Type-2 immune response in healthy animals [14]. In the current study, we demonstrated that in tumor-bearing animals, irradiation can induce lung fibrosis more easily than in healthy mice and that a Type-2–mediated immune mechanism might play an important role in RILF.

Radiation can alter the composition of the cellular immune infiltrate through the induction of cytokines such as TNF, IL-1 and IL-6 [9, 25], but only low levels of Type-1 immune cytokines were observed in the LRT group. These results may be due to failure of tumor regression in a lung-centered irradiation field and a strong Type-2 immune phenotype in our tumor-bearing mouse model. High levels of Type-2 cytokines (IL-5 and IL-13) in circulating blood have been shown to participate in both the initiation and progression of cancer [26]. The expression of high levels of GATA-3 and its corresponding signaling cascade were seen not only in tumor masses, but also in normal lung tissue from tumor-bearing mice. Thus, the persistence of tumors with a Type-2 immune phenotype was possibly related to an increased risk of pulmonary fibrosis.

Commonality between tumor environment and irradiated normal tissues has been observed. For example, cancer-induced myeloid-derived suppressor cells in peripheral blood can display the phenotypic and functional hallmarks of fibrocytes, and these cells were likely increased in response to Type-2 immune deviation [27]. Additionally, M2 macrophages and hyperactivation of TGF-β signaling contributes to EMT-associated changes such as metastasis and cancer stem cell formation, and leads to RILF during radiotherapy [28–30]. Therefore, after irradiation, tumors might deliver Type-2 cytokines or other pro-fibrogenic signals into normal lung tissue via the circulation and eventually affect the progression of normal tissue damage.

STAT1, STAT4 and STAT6 are signal transduction molecules that associate with IFN-γ, IL-12 and IL-4/IL-13 receptors, respectively [31]. Activation of STAT1, STAT4 and STAT6 is pivotal in the differentiation of Type-1 and Type-2 T-cells [31]. In our study, administration of the strong Type-1 immune adjuvant CpG-ODN reduced the expression of STAT6 and GATA-3 in the lung tissue by activating STAT1, STAT4 and T-bet. CpG-ODN has been shown in previous studies to enhance the induction of anti-tumor immune responses, but its ability to delay or stop the pathological changes of RILF has not previously been demonstrated [32–34]. It appeared that improving the Type-1 immune response might be a potential and effective means of treating RILF in tumor-bearing mice. The results of this study will be used as the basis for further studies to test the safety and clinical efficacy of radiotherapy combined with Type-1 related immunotherapy and its molecular mechanisms.

In conclusion, our data provide a scientific rationale that Type-2 immune phenotype in tumors can affect the outcome of radiation damage. Boosting Type-1 related immunity with an appropriate

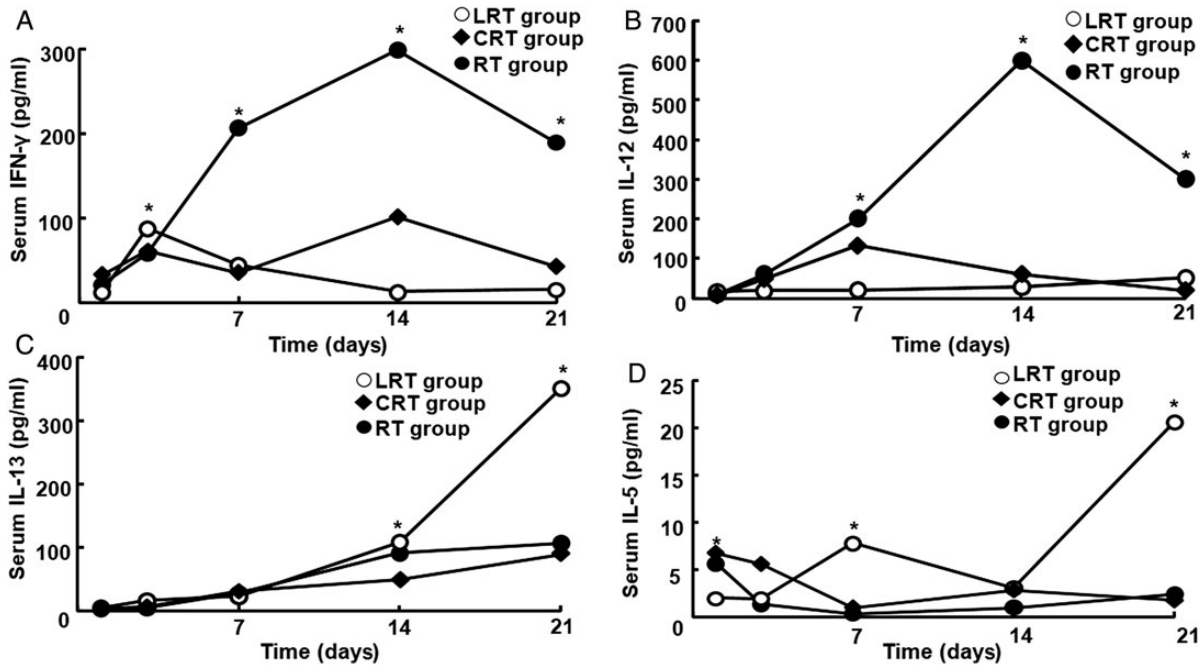

Fig. 6. Type-1 and Type-2 cytokine levels in mouse serum after irradiation. Three weeks after irradiation, IFN-γ (A) and IL-12 (B) were at maximum levels in the RT group, but their expression in serum from mice in the LRT group increased initially, then decreased rapidly and became stable. (C) The IL-13 level in serum from LRT group mice was higher than in the control RT group, and reached a maximum value. (D) IL-5 level in serum from LRT group mice was increased compared with that in the RT group. CpG-ODN treatment decreased IL-5 and IL-13 expression in the CRT group, whereas serum IL-12 and INF-γ increased at Day 7 and 14, respectively. Data are shown as mean ± SD. *$P < 0.05$.

vaccine might be possible and may create strong anti-tumor effects and normal tissue protection when effectively combined with standard cancer therapies, such as radiation. These combination treatments might play an important role in future clinical developments.

FUNDING

Funding to pay the Open Access publication charges for this article was provided by National Natural Science Foundation of China (Grant No. 81272996) and the Natural Science Foundation of Hubei Province (Grant No.2013CFA006).

REFERENCES

1. Roach M III, Gandara DR, Yuo H-S, et al. Radiation pneumonitis following combined modality therapy for lung cancer: analysis of prognostic factors. *J Clin Oncol* 1995;13:2606–12.
2. Shi A, Zhu G, Wu H, et al. Analysis of clinical and dosimetric factors associated with severe acute radiation pneumonitis in patients with locally advanced non-small cell lung cancer treated with concurrent chemotherapy and intensity-modulated radiotherapy. *Radiat Oncol* 2010;5:35.
3. Kimura T, Togami T, Takashima H, et al. Radiation pneumonitis in patients with lung and mediastinal tumours: a retrospective study of risk factors focused on pulmonary emphysema. *Br J Radiol* 2012;85:135–41.
4. Yuan X, Liao Z, Liu Z, et al. Single nucleotide polymorphism at rs1982073:T869C of the TGFβ1 gene is associated with the risk of radiation pneumonitis in patients with non–small-cell lung cancer treated with definitive radiotherapy. *J Clin Oncol* 2009;27:3370–8.
5. Marks LB, Yu X, Vujaskovic Z, et al. Radiation-induced lung injury. *Semin Radiat Oncol* 2003;13:333–45.
6. Rubin P, Johnston CJ, Williams JP, et al. A perpetual cascade of cytokines postirradiation leads to pulmonary fibrosis. *Int J Radiat Oncol Biol Phys* 1995;33:99–109.
7. Schaue D, McBride WH. Links between innate immunity and normal tissue radiobiology. *Radiat Res* 2010;173:406–17.
8. Rodemann HP, Bamberg M. Cellular basis of radiation-induced fibrosis. *Radiother Oncol* 1995;35:83–90.
9. Burnette B, Weichselbaum RR. Radiation as an immune modulator. *Semin Radiat Oncol* 2013;23:273–80.
10. Liang H, Deng L, Chmura S, et al. Radiation-induced equilibrium is a balance between tumor cell proliferation and T cell–mediated killing. *J Immunol* 2013;190:5874–81.
11. Finotto S, Neurath MF, Glickman JN, et al. Development of spontaneous airway changes consistent with human asthma in mice lacking T-bet. *Science* 2002;295:336–8.
12. Mowen KA, Glimcher LH. Signaling pathways in Th2 development. *Immunol Rev* 2004;202:203–22.
13. Wynn TA. Fibrotic disease and the T_H1/T_H2 paradigm. *Nat Rev Immunol* 2004;4:583–94.
14. Han G, Zhang H, Xie C-H, et al. Th2-like immune response in radiation-induced lung fibrosis. *Oncol Rep* 2011;26:383–8.

15. Masui Y, Asano Y, Shibata S, et al. A possible contribution of visfatin to the resolution of skin sclerosis in patients with diffuse cutaneous systemic sclerosis via a direct anti-fibrotic effect on dermal fibroblasts and Th1 polarization of the immune response. *Rheumatology* 2013;52:1239–44.
16. Grivennikov SI, Greten FR, Karin M. Immunity, inflammation, and cancer. *Cell* 2010;140:883–99.
17. Neurath MF, Finotto S. The emerging role of T cell cytokines in non-small cell lung cancer. *Cytokine Growth Factor Rev* 2012;23:315–22.
18. Ortegel JW, Staren ED, Faber LP, et al. Modulation of tumor-infiltrating lymphocyte cytolytic activity against human non–small cell lung cancer. *Lung Cancer* 2002;36:17–25.
19. Huang M, Wang J, Lee P, et al. Human non-small cell lung cancer cells express a type 2 cytokine pattern. *Cancer Res* 1995;55:3847–53.
20. Shurin MR, Lu L, Kalinski P, et al. Th1/Th2 balance in cancer, transplantation and pregnancy. *Springer Semin Immunopathol* 1999;21:339–59.
21. Patel S, Vetale S, Teli P, et al. IL-10 production in non–small cell lung carcinoma patients is regulated by ERK, P38 and COX-2. *J Cell Mol Med* 2012;16:531–44.
22. Lazarevic V, Chen X, Shim JH, et al. Transcription factor T-bet represses T_H17 differentiation by preventing Runx1-mediated activation of the gene encoding RORγt. *Nat Immunol* 2011;12:96–104.
23. Karpathiou G, Giatromanolaki A, Koukourakis MI, et al. Histological changes after radiation therapy in patients with lung cancer: a prospective study. *Anticancer Res* 2014;34:3119–24.
24. Hübner RH, Gitter W, El Mokhtari NE, et al. Standardized quantification of pulmonary fibrosis in histological samples. *BioTechniques* 2008;44:507–11. :14–7.
25. Sharma S, Stolina M, Lin Y, et al. T cell–derived IL-10 promotes lung cancer growth by suppressing both T cell and APC function. *J Immunol* 1999;163:5020–8.
26. Takeshima T, Chamoto K, Wakita D, et al. Local radiation therapy inhibits tumor growth through the generation of tumor-specific CTL: its potentiation by combination with Th1 cell therapy. *Cancer Res* 2010;70:2697–706.
27. Zhang H, Maric I, DiPrima MJ, et al. Fibrocytes represent a novel MDSC subset circulating in patients with metastatic cancer. *Blood* 2013;122:1105–13.
28. Zhang H, Han G, Liu H, et al. The development of classically and alternatively activated macrophages has different effects on the varied stages of radiation-induced pulmonary injury in mice. *J Radiat Res* 2011;52:717–26.
29. Zhou Y-C, Liu J-Y, Li J, et al. Ionizing radiation promotes migration and invasion of cancer cells through transforming growth factor-beta–mediated epithelial–mesenchymal transition. *Int J Radiat Oncol Biol Phys* 2011;81:1530–7.
30. Anscher MS. Targeting the TGF-β1 pathway to prevent normal tissue injury after cancer therapy. *Oncologist* 2010;15:350–9.
31. Krieg AM. Toll-like receptor 9 (TLR9) agonists in the treatment of cancer. *Oncogene* 2008;27:161–7.
32. Chamoto K, Takeshima T, Wakita D, et al. Combination immunotherapy with radiation and CpG-based tumor vaccination for the eradication of radio- and immuno-resistant lung carcinoma cells. *Cancer Sci* 2009;100:934–9.
33. Pernis AB, Rothman PB. JAK-STAT signaling in asthma. *J Clin Invest* 2002;109:1279–83.
34. Suzuki Y, Wakita D, Chamoto K, et al. Liposome-encapsulated CpG oligodeoxynucleotides as a potent adjuvant for inducing type 1 innate immunity. *Cancer Res* 2004;64:8754–60.